



Published in final edited form as:

Biochemistry. 2008 June 10; 47(23): 6138–6147.

## SPTLC1 Binds ABCA1 To Negatively Regulate Trafficking and Cholesterol Efflux Activity of the Transporter<sup>†</sup>

Norimasa Tamehiro<sup>‡,§,||</sup>, Suiping Zhou<sup>‡,§,||</sup>, Keiichiro Okuhira<sup>⊥</sup>, Yair Benita<sup>§</sup>, Cari E Brown<sup>‡,§</sup>, Debbie Z Zhuang<sup>‡,§</sup>, Eicke Latz<sup>#</sup>, Thorsten Hornemann<sup>+</sup>, Arnold von Eckardstein<sup>+</sup>, Ramnik J Xavier<sup>§</sup>, Mason W Freeman<sup>‡,§</sup>, and Michael L Fitzgerald<sup>\*,‡,§</sup>

*Lipid Metabolism Unit and Center for Computational and Integrative Biology, Massachusetts General Hospital, Harvard Medical School, 185 Cambridge Street, Boston, Massachusetts 02114, National Institute of Health Sciences, Setagaya-ku, Tokyo, Japan, University of Massachusetts Medical School, 55 Lake Avenue, North Worcester, Massachusetts 01605, and Institute for Clinical Chemistry, University Hospital Zurich, Ramistrasse 100, CH-8091 Zurich, Switzerland*<sup>‡</sup>*Lipid Metabolism Unit, Massachusetts General Hospital, Harvard Medical School.*<sup>§</sup>*Center for Computational and Integrative Biology, Massachusetts General Hospital, Harvard Medical School. National Institute of Health Sciences.*<sup>#</sup>*University of Massachusetts Medical School.*<sup>+</sup>*University Hospital Zurich.*

### Abstract

ABCA1 transport of cholesterol and phospholipids to nascent HDL particles plays a central role in lipoprotein metabolism and macrophage cholesterol homeostasis. ABCA1 activity is regulated both at the transcriptional level and at the post-translational level. To explore mechanisms involved in the post-translational regulation of the transporter, we have used affinity purification and mass spectrometry to identify proteins that bind ABCA1 and influence its activity. Previously, we demonstrated that an interaction between  $\beta$ 1-syntrophin stimulated ABCA1 activity, at least in part, by slowing the degradation of the transporter. This work demonstrates that one subunit of the serine palmitoyltransferase enzyme, SPTLC1, but not subunit 2 (SPTLC2), is copurified with ABCA1 and negatively regulates its function. In human THP-1 macrophages and in mouse liver, the ABCA1-SPTLC1 complex was detected by co-immunoprecipitation, demonstrating that the interaction occurs in cellular settings where ABCA1 activity is critical for HDL genesis. Pharmacologic inhibition of SPTLC1 with myriocin, which resulted in the disruption of the SPTLC1-ABCA1 complex, and siRNA knockdown of SPTLC1 expression both stimulated ABCA1 efflux by nearly 60% ( $p < 0.05$ ). In contrast, dominant-negative mutants of SPTLC1 inhibited ABCA1 efflux, indicating that a reduced level of sphingomyelin synthesis could not explain the effect of myriocin on ABCA1 activity. In 293 cells, the SPTLC1 inhibition of ABCA1 activity led to the blockade of the exit of ABCA1 from the endoplasmic reticulum. In contrast, myriocin treatment of macrophages increased the level of cell surface ABCA1. In composite, these results indicate that the physical interaction of ABCA1 and SPTLC1 results in reduction of ABCA1 activity and that inhibition of this interaction produces enhanced cholesterol efflux.

Disruption of cellular cholesterol homeostasis leads to a variety of pathological conditions, including cardiovascular disease (1). Active efflux of cholesterol to extracellular

<sup>†</sup>This work was supported by National Institutes of Health Grants HL074136 (M.L.F.) and R24RR020345 (M.W.F.).

\*To whom correspondence should be addressed: Lipid Metabolism Unit, Center for Computational and Integrative Biology, Massachusetts General Hospital, Harvard Medical School, 185 Cambridge St., Boston, MA 02114. Telephone: (617) 726-1645. Fax: (617) 643-3328. mfitzgerald@ccib.mgh.harvard.edu.

<sup>||</sup>These authors contributed equally to this work.

apolipoproteins, primarily apolipoprotein A-I (apoA-I),<sup>1</sup> allows cells to rid themselves of excess cholesterol. The physiologic importance of this process is clear since patients with Tangier disease carry loss-of-function mutations in the ABCA1 transporter that eliminate apoA-I-mediated cholesterol efflux (2-5). This condition is associated with a near absence of circulating HDL and increased risk for the development of atherosclerotic vascular disease (6-8). Tangier patients also suffer from peripheral neuropathies, a feature of the disease that to date has defied mechanistic explanation (9).

ABCA1-mediated cholesterol efflux is highly regulated at both the transcriptional and post-translational levels. For ABCA1, we have shown how protein-protein interactions are important in the post-translational regulation of the transporter. By analyzing a mutation carried by a Tangier patient that deletes the 46 highly conserved C-terminal amino acids of ABCA1, we identified a VFVNFA motif between amino acids -41 and -46 that is critical for efflux function and the ability of ABCA1 to bind apoA-I (10,11). This motif can act in trans to inhibit ABCA1 efflux activity and the binding of apoA-I, suggesting it may represent a novel protein-protein interaction domain. The final three amino acids of ABCA1 also conform to the consensus sequence of a class I PDZ protein binding motif. These C-terminal motifs are bound by cytoplasmic proteins that contain one or more copies of the 90-amino acid PDZ domain. Thus, to identify proteins that bind ABCA1, wild-type ABCA1 and C-terminally mutated forms of ABCA1 were affinity purified, and mass spectrometry was used to identify proteins that were differentially copurified with ABCA1 and the mutant transporters (12). Utrophin, as well as  $\beta$ 1- and  $\beta$ 2-syntrophin, both PDZ proteins, was prominent among the proteins that are copurified with wild-type ABCA1 but not with a mutant ABCA1 transporter lacking its last 40 amino acids. The  $\beta$ 1-syntrophin interaction was shown to positively regulate ABCA1 efflux in primary human fibroblasts and mouse macrophages, and coexpression studies in 293 cells indicated  $\beta$ 1-syntrophin stabilizes newly translated ABCA1 by altering the cellular distribution of the transporter and increasing its level of cell surface expression.

Here we have further mapped the network of ABCA1 protein-protein interactions identified by the affinity purification-mass spectrometry approach. These screens identified SPTLC1 as a potential ABCA1 binding protein. Given SPTLC1's involvement in sphingomyelin synthesis, and the latter's positive correlation with atherosclerotic vascular disease, we further investigated the relevance of SPTLC1's binding to ABCA1 (13,14). Co-immunoprecipitation assays detected the ABCA1-SPTLC1 complex in liver tissue and in macrophages, the critical cellular environments in which ABCA1 functions to maintain HDL levels and inhibit atherosclerotic progression (8,15). Myriocin, an SPTLC1/2 inhibitor, and siRNA inhibition of SPTLC1 both stimulated ABCA1 efflux activity in primary human fibroblasts and mouse macrophages. Myriocin disrupted the ABCA1-SPTLC1 complex, suggesting that its effect on

---

<sup>1</sup>Abbreviations

<b>ABCA1</b>	ATP cassette binding transporter A1
<b>apoA-I</b>	apolipoprotein A-I
<b>ER</b>	endoplasmic reticulum
<b>HDL</b>	high-density lipoprotein
<b>PARD3</b>	partitioning-defective protein 3 homologue
<b>SPT</b>	serine palmitoyltransferase.

ABCA1 efflux might not depend on its inhibition of sphingomyelin synthesis. This hypothesis was supported by the finding that dominant-negative SPTLC1 mutants, which also inhibit sphingolipid production, produced an inhibition of ABCA1 activity. Although the mechanism by which SPTLC1 inhibited ABCA1 cholesterol efflux did not appear to require SPTLC1 serine palmitoyltransferase activity, it was associated with a block in the exit of ABCA1 from the endoplasmic reticulum. In aggregate, these studies show that SPTLC1 can physically and functionally interact with ABCA1, leading to the inhibition of the latter's cholesterol efflux activity.

## MATERIALS AND METHODS

### Reagents and DNA Constructs

The following reagents were purchased from the indicated suppliers: myriocin, oleylethanolamide, and sphingomyelin (Biomol); anti-FLAG antibody agarose beads (Sigma); anti-SPTLC1 mouse monoclonal antibody (BD Transduction Laboratories); anti-SPTLC2 rabbit polyclonal antibody (Abgent); apoA-I (Biode-sign); radionucleotides (PerkinElmer); and TransSignal PDZ Domain Arrays (Panomics). Clones were obtained from the indicated suppliers for the following human cDNAs: SPTLC1 and SPTLC2 (OpenBiosystems), PARD3 (Origene), and pDsRed2-ER (BD Biosciences). The cDNAs were sequenced on both strands to confirm they were full-length and did not contain mutations. As necessary, cDNAs were transferred to a mammalian expression vector (pcDNA3.1) using standard cloning techniques to produce wild-type and N-terminally hemagglutinin- and FLAG-tagged versions of the cDNAs (HA, YPYDVPDYA; FLAG, DYKDDDDK). The GFP- and FLAG-tagged ABCA1 constructs and the rabbit anti-SPTLC1 antibody have been previously described, and the SPTLC1-C133W and -C133Y mutants were generated by overlap PCR mutagenesis (11,16).

### Mass Spectrometry

The FLAG-tagged ABCA1 transporter with the VFVNFA motif mutated to alanines (FLAG-ABCA1-A6) was affinity purified, and the copurifying proteins were identified by mass spectrometry as previously described for the FLAG-ABCA1- $\Delta$ 40 mutant (12). In brief, HEK-293-EBNA-T cells ( $5.6 \times 10^8$  cells) were transfected with the FLAG-ABCA1-A6 mutant cDNA (750  $\mu$ g of DNA/ 1.875 mL of Lipofectamine 2000). After the cells had been cultured for 24 h, a 15000g, postnuclear membrane pellet was prepared using a hypotonic buffer [250 mM sucrose and 10 mM HEPES (pH 7.5) with protease inhibitor cocktail]. The 15000g membrane pellet was solubilized [0.75% CHAPS, 50 mM HEPES (pH 7.0), 140 mM NaCl, 1 mg/mL phosphatidylcholine, 10% glycerol, 3 mM MgCl<sub>2</sub>, and 5mM  $\beta$ -mercaptoethanol], and the FLAG-ABCA1-A6 mutant was purified using an anti-FLAG antibody affinity column. Proteins that coeluted with the FLAG-ABCA1-A6 mutant were identified on a LCQ DECA XP plus mass spectrometer (Thermo Electron) and compared to the proteins that co-eluted with wild-type FLAG-ABCA1 and the FLAG-ABCA1- $\Delta$ 40 mutant. Additional screens using PDZ protein arrays, to be published elsewhere, identified a SPTLC1 interaction with the partitioning-defective protein 3 homologue (PARD3). Here, the SPTLC1—PARD3 interaction was used as a control to demonstrate that myriocin specifically disrupted the ABCA1—SPTLC1 interaction.

### Immunological Assays

Immunoprecipitations were used to confirm the physical interaction of ABCA1 and SPTLC1 in lysates from THP-1 macrophages and mouse liver. THP-1 cells ( $3 \times 10^7$  cells/10 cm dish) were differentiated with phorbol 12-myristate 13-acetate (PMA, 0.1  $\mu$ M, 72 h); the LXR agonist T0-901317 was then added to maximize ABCA1 expression (10  $\mu$ M, 48 h) or not (DMSO vehicle), and cell lysates were prepared with Triton X-100 buffer [1% Triton X-100, 140 mM NaCl, 3 mM MgCl<sub>2</sub>, 10% glycerol, 50 mM HEPES (pH 7.0), and protease inhibitor cocktail,

at 2 mL/plate]. Precleared lysates (1 mg of total protein) were incubated with 50  $\mu$ g of a Pro-A-purified anti-ABCA1 rabbit antibody or an equivalent amount of normal rabbit IgG, and immune complexes were captured with TrueBlot anti-rabbit Ig beads (eBioscience) and washed as previously described (12). After being separated via SDS—PAGE and transferred to nitrocellulose, SPTLC1 was detected using an anti-SPTLC1 mouse monoclonal antibody and a secondary TrueBlot anti-mouse antibody. Liver immunoprecipitations were conducted likewise expect that the Triton-X 100 lysates were prepared from a 15000g membrane pellet prepared as described above and 5 mg of total protein was used. For 293 cell experiments, FLAG-ABCA1 or FLAG-SPTLC1 was precipitated using anti-FLAG antibody beads, and the untagged SPTLC1 or ABCA1, respectively, that coprecipitated was detected by immunoblotting. The effect of SPTLC1 expression on the cell surface levels of ABCA1 in 293 cells was determined by radio-immunodetection of the FLAG epitope in the first large extracellular loop of ABCA1 as previously described (17). To assess endogenous ABCA1 at the cell surface in bone marrow and THP-1 macrophages, cell surface proteins were selectively biotinylated using the membrane impermeable Sulfo-NHS-Biotin reagent (Pierce), biotinylated proteins were purified using NeutrAvidin beads (Pierce), and the level of biotinylated ABCA1 was determined by Western blotting and densitometry.

### Cholesterol Efflux Assays, Myriocin, and siRNA Inhibition of SPTLC1

Cholesterol efflux assays were carried out as previously described (11). In brief, 293-EBNA-T cells were seeded into 24-well poly-D-lysine-coated tissue culture plates at a density of 100000 cells/well and 72 h later were transfected in triplicate with empty vector or the indicated cDNAs using Lipofectamine 2000 (Invitrogen). In assays involving transfection of multiple cDNAs, empty vector was used to maintain an equal amount of transfected DNA. Twenty-four hours post-transfection, the cells were incubated with 0.5  $\mu$ Ci/mL [ $^3$ H]cholesterol in complete medium (10% FBS/DMEM) for 24 h. Non-cell-associated cholesterol was removed by two washes with 1  $\times$  PBS, a 2 h incubation in medium at 37  $^{\circ}$ C, and two additional washes in 1  $\times$  PBS. The cells were further incubated in medium alone (2 mg/mL fatty acid-free BSA/DMEM) or in medium with 10  $\mu$ g/mL delipidated apoA-I for 20 h. Medium was collected from the cells and cleared of debris by an 800g spin for 10 min. To calculate the rates of total cholesterol uptake and efflux, the cell layers were dissolved in 0.1 N NaOH, and the amount of radioactivity in the media and cell lysates was measured by scintillation counting. ApoA-I-dependent cholesterol efflux was expressed as the difference in the percentage of efflux [medium counts per minute/(medium + cell counts per minute)  $\times$  100] for the apoA-I-treated cells minus the percentage of efflux from the cells treated with medium alone. Efflux measurements in primary 1056 human fibroblasts and mouse bone marrow-derived macrophages were conducted as previously described (12). For these experiments, the expression of ABCA1 was induced by the treatment of the cells with 10  $\mu$ g/mL ethanolic cholesterol in addition to the radiolabel, and cells were exposed either to vehicle (DMSO) or to 10  $\mu$ M myriocin or oleylethanolamide during the apoA-I incubation step. For siRNA knockdown of SPTLC1, primary screening of OpenBiosystems lentiviral constructs targeting human SPTLC1 showed clone NM\_006415.2-1294s1c1 had the greatest efficacy in reducing the level of expression of SPTLC1 protein. After selection in puromycin (4  $\mu$ g/ml, 48 h postinfection for 72 h), primary human fibroblasts expressing the SPTLC1 siRNA or a nontargeting control siRNA were assayed for SPTLC1 protein expression and ABCA1 efflux activity. Endogenous SPTLC1 was also suppressed in THP-1 macrophages using the lentiviral vectors, and cell surface ABCA1 levels were determined by the biotinylation assay after differentiation of the cells with PMA as described above. Levels of ABCA1 mRNA were determined by reverse transcription quantitative PCR assays as previously described (12). Cell viability was determined using the MTT enzymatic assay as described by the manufacturer (Biotium).

## Subcellular Distribution of ABCA1

The cellular distributions of GFP-tagged ABCA1 and the GFP-ABCA1- $\Delta$ 46 mutant were determined relative to the Alexa Fluor conjugate of the B subunit of cholera toxin (CTXB) and the ER-Tracker Blue-White DPX probe (Molecular Probes) using vital confocal microscopy. 293 cells grown on glass-bottomed 35 mm dishes (Mattek) and transfected with the GFP-ABCA1 constructs were incubated with CTXB (5  $\mu$ g/mL, 4 °C) for 10 min and directly imaged to assess cell surface CTXB binding. The cells were then incubated at 37 °C for 30 min to allow endocytosis and trafficking of the CTXB to the Golgi apparatus and again imaged. For localization of the GFP-ABCA1 constructs relative to the endoplasmic reticulum (ER), the cells were incubated with the Blue-White DPX probe (100 nM, 37 °C for 30 min) and imaged directly. Images were captured on an inverted Axiovert 100-M microscope equipped with a Leica SP2 AOBS scanning unit and a 1.4 NA 63 $\times$  apochromat objective. To determine the effect of SPTLC1 expression on the cellular localization of GFP-ABCA1 relative to the ER, cells were transfected with GFP-ABCA1 cDNA and the pDsRed2-ER vector (BD Biosciences), which expresses a fusion protein of the DsRed fluorescent protein with the C-terminal ER retention signal of calreticulin, either alone or in the presence of the SPTLC1 cDNA. The localization of SPTLC1 was assessed using a HA-SPTLC1 construct and an anti-HA antibody (Covance). The DsRed-transfected cells were imaged on a Leica TCS SP confocal microscope using a 63 $\times$  oil immersion lens.

ABCA1 protein was fractionated by douncing 293 cells expressing ABCA1 with or without SPTLC1 in hypotonic buffer, and a 30000g membrane pellet (30P) was recovered. The pellet was resuspended (0.425 mL of 12.5% sucrose buffer) and overlaid on a discontinuous sucrose gradient (0.319 mL of 26%, 0.319 mL of 34%, 0.638 mL of 42%, 1.275 mL of 46%, 0.85 mL of 50%, and 0.638 mL of 54 and 60% sucrose in buffer). The gradient was spun at 170000g for 16 h, and fractions were collected by needle puncture from the bottom of the tube. Fractions were diluted with 3 volumes of HEPES buffer and centrifuged for 2.5 h at 100000g, and membrane pellets were resuspended in a constant volume of SDS buffer for analysis by immunoblotting.

## Statistical Analysis

Data from the cholesterol efflux assays were found to have equal variance and were further compared by a two-tailed Student's *t* test using SigmaStat. Statistical significance was defined by a *P* of <0.05.

## RESULTS

### Demonstration of an ABCA1-SPTLC1 Complex at Physiologic Expression Levels in Human THP-1 Macrophages and Mouse Liver

We have developed screens for ABCA1 protein-protein interactions. Initially, ABCA1, as well as two ABCA1 transporters with C-terminal mutations in suspected protein-protein interaction motifs, was purified by affinity chromatography out of human 293 cells, and the proteins that interacted with ABCA1 and the mutants were identified by mass spectrometry (12). One mutant ( $\Delta$ 40) deletes the PDZ motif but leaves the VFVNFA motif intact, and a second transporter selectively mutates the VFVNFA motif to alanines (ABCA1-A6). Significantly, analysis of the A6 and  $\Delta$ 40 data sets suggested mutation of these motifs modulated the interaction of ABCA1 with a number of proteins that, like ABCA1, have C-termini that could also bind PDZ proteins (see Table 1 of the Supporting Information). Of these interactions, SPTLC1, but not its heterodimeric partner, SPTLC2, was copurified with ABCA1, and more than twice as many peptide identifications were found for SPTLC1 in the sample from the  $\Delta$ 40 mutant. Similarly, 75% more SPTLC1 peptide identifications were found in the ABCA1-A6 mutant sample.

These results indicated SPTLC1 has the potential to interact with ABCA1 but that the interaction does not depend upon an intact ABCA1 C-terminus.

Given the reported pro-atherosclerotic role of SPTLC1, we focused our study on the functional significance of the interaction of SPTLC1 with ABCA1. Because ABCA1 function in macrophages and in the liver is critical for maintaining plasma HDL levels and preventing atherosclerosis, we first tested whether the ABCA1-SPTLC1 complex could be detected at physiologic expression levels of these proteins in macrophages and in the liver. Western blots showed that SPTLC1, like ABCA1, was strongly expressed in macrophages and in the liver, indicating that formation of a complex between these proteins was possible (Figure 1A,B). We then generated protein lysates from human THP-1 macrophages differentiated with PMA and stimulated them with the LXR agonist T0-901317 or not. Treatment of these cells with T0-901317 maximizes ABCA1 expression and efflux activity but does not significantly alter SPTLC1 expression (data not shown). ABCA1 was immunoprecipitated from these lysates with a rabbit polyclonal antibody, and after separation via SDS-PAGE and transfer to nitrocellulose, an anti-SPTLC1 antibody was used to immunoblot the membranes for the presence of SPTLC1. In the sample from cells differentiated with only PMA, a small amount of SPTLC1 was detected in the ABCA1 precipitate, while the amount of SPTLC1 was dramatically increased in the ABCA1 precipitate from differentiated cells treated with LXR agonist T0-901317 (Figure 1A). In contrast, in a precipitate generated by incubating an equivalent amount of nonimmune IgG with a lysate from differentiated and T0-901317-treated cells, little or no SPTLC1 was detected, demonstrating the specificity of the ABCA1 precipitations. Additional ABCA1 immunoprecipitations were carried out using protein lysates from mouse liver, and again SPTLC1 prominently coprecipitated with ABCA1 (Figure 1B, top panel). Because of the slight cross reactivity of the secondary antibody to the IgG precipitate in this assay, we conducted converse precipitations using mouse liver lysates and an anti-SPTLC1 antibody. In this case, probing for ABCA1 detected the transporter in the SPTLC1 precipitate, but not in the IgG control precipitate (Figure 1B, bottom panel). In composite, these results demonstrated the presence of the ABCA1-SPTLC1 complex in cells and tissues where ABCA1 efflux activity is critical for HDL biogenesis and preventing atherosclerosis. While further work is underway to characterize the functional importance of the other novel protein interactions identified in the MS screens, this report focuses on the SPTLC1-ABCA1 interaction, which we chose to explore initially because of the relevance of sphingolipid synthesis to atherosclerosis.

### **Inhibition of SPTLC1 with Myriocin or by siRNA Knock-down Increases the Rate of ABCA1 Efflux**

Having demonstrated the ABCA1-SPTLC1 complex could be detected in cells expressing naturally occurring levels of the proteins, and since these cells represent the tissues most relevant to the known roles of ABCA1 *in vivo*, we next tested whether SPTLC1 function might influence ABCA1 efflux activity. This possibility was tested using primary human fibroblasts or mouse bone marrow-derived macrophages, which also express both ABCA1 and SPTLC1 (Figure 2A,C). Fibroblasts were treated with myriocin, a specific inhibitor of the SPTLC1/2 enzyme, and the rate of cholesterol efflux to apoA-I was measured. It was found that myriocin treatment of these cells increased the rate of efflux to apoA-I by more than 50% (Figure 2A). Lentiviral mediated knockdown was used to efficiently suppress SPTLC1 expression in these cells to perform an independent test of SPTLC1's influence on ABCA1 function (Figure 2B). Compared to fibroblasts infected with a control lentivirus expressing a nontargeting small hairpin RNA, cells expressing the siRNA targeting SPTLC1 exhibited significantly greater apoA-I-dependent cholesterol efflux. These findings indicated that SPTLC1 negatively regulated ABCA1 transport function and suggested that this was accomplished either via

inhibition of sphingolipid synthesis or through some direct effect on SPTLC1's interaction with the transporter.

As with fibroblasts, treatment of mouse bone marrow macrophages with myriocin significantly increased the rate of apoA-I-dependent efflux by more than 50% (Figure 2C). Because ABCA1 moves both cholesterol and phospholipid onto apoA-I, we further tested whether myriocin treatment of the mouse macrophages also stimulated the efflux of phosphatidylcholine, which was found to be the case (Figure 2C). The myriocin stimulation of ABCA1 efflux was specific in that oleylethanolamide, a related long chain base ceramidase inhibitor, did not stimulate apoA-I-mediated efflux activity of either cholesterol or phosphatidylcholine (Figure 2C). Because myriocin treatment may have been reducing cellular sphingomyelin levels, which can bind cholesterol and possibly sequester it from the ABCA1 efflux pathway(18,19), we tested whether adding exogenous sphingomyelin to the cells could block the myriocin stimulation of ABCA1 efflux. This was found not to be the case (data not shown). This indicated that disruption of SPTLC1 function was likely not stimulating ABCA1 efflux by decreasing cellular sphingo-myelin levels. Thus, we speculated that myriocin may be capable of disrupting the ABCA1-SPTLC1 complex and that the formation of such a complex might be required for SPTLC1's inhibition of ABCA1 activity. Substantiating this hypothesis, when ABCA1 and SPTLC1 were co-expressed in 293 cells, the complex they form could be dissociated in the presence of myriocin (Figure 2D, top panel). In converse immunoprecipitations that exploited a FLAG-SPTLC1 construct, we tested whether the myriocin disruption of the ABCA1-SPTLC1 complex was specific. As a control, we analyzed the interaction of SPTLC1 with PARD3, a PDZ protein involved in cell polarity that we have identified in additional protein interaction screens to be published elsewhere. This experiment confirmed that myriocin disrupted the ABCA1-SPTLC1 complex (Figure 2D, middle panel). The myriocin disruption of the ABCA1-SPTLC1 complex was specific since equal if not greater amounts of PARD3 associated with SPTLC1 in myriocin-treated cells (Figure 2D, bottom panels). In aggregate, our data indicate myriocin stimulates ABCA1 efflux activity and can selectively disrupt the ABCA1-SPTLC1 complex.

### **Co-Expression of SPTLC1, as Well as Dominant-Negative SPTLC1 Mutants, Represses ABCA1 Cholesterol Efflux**

The myriocin experiments suggested that the formation of a protein complex with ABCA1 was central to the inhibitory activity of SPTLC1 on ABCA1 function, but they did not preclude a role for sphingomyelin synthesis in this process. When SPTLC1 was overexpressed in 293ET cells along with ABCA1, the rate of cholesterol efflux was reduced by more than 50%, establishing that bidirectional changes in wild-type SPTLC1 levels produced equivalent but opposite effects on ABCA1 activity (Figure 3A). This finding also enabled us to explore the issue of the dependence of this regulatory activity on sphingolipid synthesis. Using two well-characterized SPTLC1 mutants that are known to have a dominant-negative effect on sphingolipid synthesis (SPTLC1-C133W and SPTLC1-C133Y) (20, 21), we tested the hypothesis that overexpression of the SPTLC1 protein, but not its functional enzymatic activity, was necessary for the inhibitory effect on ABCA1. As anticipated, expression of either the SPTLC1-C133W or -C133Y mutant produced equally great or greater inhibition of ABCA1 efflux activity as wild-type SPTLC1, despite their documented inhibitory effect on serine palmitoyltransferase activity (Figure 3A). Thus, the ability of the C133W and C133Y mutants to inhibit efflux established that the reduction of ABCA1 efflux activity by overexpression of SPTLC1 in 293 cells was not dependent upon an increased level of synthesis of sphingomyelin.

In the experiments described above, SPTLC1 and the SPTLC1 mutants were transfected into cells that were not transfected with SPTLC2. Because SPTLC2 is bound and stabilized by both SPTLC1 and the dominant-negative mutants, this raised the question of whether the inhibition

of ABCA1 efflux would occur in the presence of SPTLC1's known binding partner, SPTLC2. To explore this issue, we conducted additional cholesterol efflux experiments in which ABCA1 was co-expressed with SPTLC1 and the C133Y mutant in the presence or absence of SPTLC2. Coexpression of SPTLC1 or the C133Y mutant with SPTLC2 generated equally great if not greater inhibition of ABCA1 efflux (Figure 3B). Thus, ABCA1 inhibition by SPTLC1 can occur in settings where the subunits that form the serine palmitoyltransferase holoenzyme are both present.

### **SPTLC1 Expression or Deletion of the 46 C-Terminal Amino Acids of ABCA1 Inhibits the Exit of ABCA1 from the Endoplasmic Reticulum**

Given the fact that SPTLC1 localizes to the endoplasmic reticulum, we hypothesized that its effect on cholesterol efflux might be secondary to an influence on the movement of ABCA1 out of this organelle. Additionally, because we have previously shown that deletion of the 46 ABCA1 C-terminal amino acids significantly blocked cell surface expression of the transporter, we speculated that the C-terminus of ABCA1 might be required for the transporter to exit the ER. To explore these possibilities, vital confocal microscopy was first used to assess the trafficking defect of the ABCA1- $\Delta$ 46 mutant in 293 cells by localizing a GFP-tagged version of this mutant relative to an Alexa Fluor conjugate of cholera toxin B (CTXB). At 4 °C, CTXB marks the cell surface via an interaction with gangliosides but is not internalized, and under these conditions, wild-type ABCA1 prominently colocalized with CTXB whereas the  $\Delta$ 46 mutant did not (Figure 4A). Warming the cells to 37 °C allows the bound CTXB to move to the Golgi apparatus, and under these conditions, the internal pool of wild-type ABCA1 again significantly colocalized with CTXB in the Golgi apparatus (Figure 4A). In contrast, the ABCA1- $\Delta$ 46 mutant still did not localize with the internalized CTXB pool. Additional experiments, however, showed the ABCA1- $\Delta$ 46 mutant strongly colocalized with a dapoxy dye that marks the endoplasmic reticulum (Figure 4B). Thus, loss of the 46 ABCA1 C-terminal amino acids, which encode the VFVNFA motif as well as the PDZ binding motif, traps ABCA1 in the endoplasmic reticulum, the organelle where SPTLC1 resides.

To test if SPTLC1 could negatively regulate ABCA1 trafficking, we first compared 293 cells transfected with GFP-ABCA1 alone or in the presence of SPTLC1. As opposed to the strong cell surface distribution of ABCA1 when expressed alone, in cells cotransfected with SPTLC1 the fluorescence of GFP-ABCA1 was found in a more perinuclear distribution, suggesting SPTLC1 had reduced the cell surface distribution of ABCA1 (Figure 1 of the Supporting Information). A radio-immunoassay that quantifies the amount of FLAG-tagged ABCA1 at the cell surface confirmed SPTLC1 co-expression significantly reduced the level of cell surface expression of ABCA1, nearly to the extent caused by the ABCA1  $\Delta$ 46 mutation (Figure 4C). Whether SPTLC1 could influence levels of cell surface ABCA1 in a physiologic setting was further tested by treating mouse bone marrow macrophages with the SPTLC1 inhibitor myriocin. Immunofluorescent staining of nonpermeabilized cells indicated myriocin treatment had increased the amount of cell surface ABCA1 (Figure 4D, left panels). This result was confirmed by selectively biotinylating cell surface proteins and determining the amount of biotinylated ABCA1 after NeutrAvidin isolation of the biotinylated proteins (Figure 4D, right panels). Densitometry of the biotinylated ABCA1 showed myriocin increased the level of macrophage cell surface ABCA1 by approximately 30%, in spite of a slight drop in the level of total ABCA1 protein. We tested whether the myriocin stimulation of cell surface ABCA1 was dependent upon SPTLC1 by knocking down SPTLC1 in THP-1 macrophages using the lentiviral siRNA construct (approximately 80% SPTLC1 knockdown). In control cells, myriocin again was found to increase the level of cell surface ABCA1, while in the cells expressing the siRNA targeting SPTLC1, the level of basal cell surface ABCA1 was increased and the ability of myriocin to stimulate cell surface ABCA1 was blunted (Figure 4E). As with the mouse bone marrow macrophages, these changes in THP-1 cell surface ABCA1 occurred



despite little change in the total ABCA1 protein level. Interestingly, in these studies, myriocin was found to stimulate ABCA1 message levels, although it did not strongly affect total ABCA1 protein levels (Figure 2 of the Supporting Information), an effect similar to that which has been previously reported for the interaction of ABCA1 with the HIV nef protein (22). In aggregate, these data indicate SPTLC1 negatively regulates cell surface ABCA1 levels by a mechanism that did not increase total ABCA1 protein levels.

Given SPTLC1 could regulate cell surface ABCA1 levels, we tested whether this was through a mechanism that regulated the exit of ABCA1 from the ER. Confocal microscopy was used to localize GFP-ABCA1 relative to SPTLC1 and a DsRed fusion protein targeted to the ER with a C-terminal KDEL sequence. By this analysis, GFP-ABCA1 significantly colocalized with the DsRed ER signal in cells expressing SPTLC1 (Figure 5A, bottom panels), which was not found to be the case for the cells expressing only GFP-ABCA1 and the DsRed construct (Figure 5A, top panels). Furthermore, localization of SPTLC1 relative to the DsRed construct confirmed it was prominently distributed to the ER along with the trapped GFP-ABCA1 (Figure 5B). This effect of SPTLC1 on ABCA1 trafficking was specific in that co-expression of SPTLC1 with the NaP<sub>i</sub> transporter, another transmembrane protein, did not affect the latter's cellular localization (Figure 5C). Additionally, the trapping of ABCA1 in the ER by SPTLC1 could not be explained by a generalized toxic effect of SPTLC1 expression since MTT assays showed no differences in cell viability after transfection with the SPTLC1 cDNA (Figure 3 of the Supporting Information). Finally, sucrose density gradients and ultracentrifugation were also used to analyze how SPTLC1 affects ABCA1 trafficking. These experiments confirmed the microscopy results in that SPTLC1 induced a redistribution of ABCA1 to the ER enriched fractions containing SPTLC1 (Figure 5D). In aggregate, these results indicate that the inhibition of ABCA1 efflux and cell surface levels of ABCA1 by SPTLC1 was associated with a prominent relocalization of ABCA1 to the ER.

## DISCUSSION

Using a proteomic approach, we have identified a protein-protein interaction that involves ABCA1 and SPTLC1. The physiological relevance of this interaction was established using immunoprecipitation, which confirmed the existence of the ABCA1-SPTLC1 complex in human macrophages and mouse liver. The interaction between ABCA1 and SPTLC1 negatively regulates ABCA1 efflux activity, as shown by myriocin inhibition of SPTLC1 and knockdown of SPTLC1 expression, both of which resulted in the stimulation of cholesterol and phospholipid efflux from primary human fibroblasts and mouse macrophages. Conversely, an increased level of expression of SPTLC1 reduced ABCA1 efflux activity by a mechanism that did not require serine palmitoyltransferase enzymatic activity, and this was associated with trapping of ABCA1 in the endoplasmic reticulum. Taken together, these results indicate SPTLC1 suppresses ABCA1 function in tissues and cells where ABCA1 efflux function is critical for HDL and macrophage cholesterol homeostasis.

The ability of SPTLC1 to block the exit of ABCA1 from the endoplasmic reticulum was of interest since we have previously shown that a protein-protein interaction between ABCA1 and  $\beta$ 1-syntrophin enhances ABCA1 cholesterol efflux by stabilizing newly translated ABCA1 protein and facilitating its expression at the cell surface. Cell surface expression of ABCA1 permits the transporter to transfer cholesterol and phospholipid to apoA-I, which is present in the extracellular environment (23,24).  $\beta$ 1-Syntrophin binds ABCA1 through the PDZ motif in the ABCA1 C-terminal domain, and the positive effect that  $\beta$  1-syntrophin has on the trafficking of ABCA1 likely is mediated by the ability of  $\beta$  1-syntrophin to recruit utrophin, a cytoskeletal binding protein, to the ABCA1 complex (12,25,26). Our mass spectrometry screens showed that when either the ABCA1 C-terminal PDZ or the VFNFA motifs are mutated, the binding of utrophin to ABCA1 is strongly disrupted. Likewise, other

factors with the potential to affect ABCA1 trafficking and its interaction with the cytoskeletal elements, such as MAP1B, can no longer interact with ABCA1 when either of the C-terminal protein-protein interaction motifs is mutated. Coupled with our demonstration that the ABCA1- $\Delta$ 46 mutant is trapped in the ER, these results indicate protein interactions with the C-terminal domain of ABCA1 play a positive role in the trafficking and efflux function of ABCA1. In contrast, the interaction of ABCA1 with SPTLC1 is not disrupted by mutation of this C-terminal domain, and SPTLC1 is able to trap wild-type ABCA1 in the ER. In composite, our results suggest a model in which the SPTLC1-ABCA1 interaction keeps the transporter sequestered in the endoplasmic reticulum, reducing efflux activity, whereas protein-protein interactions with the C-terminus of ABCA1 are necessary for the trafficking of ABCA1 out of the ER and onto the cell surface.

Why would SPTLC1 act as a negative regulator of ABCA1 function? SPTLC1 in concert with SPTLC2 catalyzes the condensation of serine and palmitoyl-CoA to form 3-keto-dihydroshingosine, the initial intermediate in the biosynthetic pathway leading to sphingomyelin, a substrate of ABCA1 efflux activity (27). Sphingomyelin is a key cellular lipid that can form a complex with cholesterol during the formation of new membrane bilayers and more specialized lipid raft subdomains. New membrane synthesis and the formation of lipid rafts increase the demand for cellular cholesterol, sphingomyelin, and other phospholipids. Thus, the ability of SPTLC1 to inhibit ABCA1 efflux function may represent a negative regulatory mechanism for maximizing cellular cholesterol and phospholipid levels when the demand for membrane synthesis is high (28,29). How these positive and negative binding interactions are regulated will require further research. However, it is interesting to note that in yeast SPTLC1 has been shown to play an important role in responding to ER stress and activating the unfolded protein response (UPR) pathway (30). In mammalian cells, the role of SPTLC1 in regulating the UPR has not been investigated, but it is known that this signaling system is used under normal physiologic conditions to maximize ER membrane synthesis and secretory capacity (31). Moreover, a series of studies has shown that when macrophages become pathologically engorged with free cholesterol, the UPR pathway is activated and this is associated with a suppression of ABCA1 activity (32). Thus, a focus of our current research is to determine whether the SPTLC1 inhibition of ABCA1 may involve activation of the UPR pathway.

In conclusion, we have used mass spectrometry to identify a rich network of protein interactions in which ABCA1 and SPTLC1 may engage. Our results show ABCA1 and SPTLC1 can physically interact and that SPTLC1 negatively regulates cholesterol efflux, which indicates the utility of this proteomic approach. It is particularly interesting that myriocin inhibition of SPTLC1 was found to stimulate macrophage cholesterol efflux. Because macrophage cholesterol efflux is important for ABCA1's anti-atherosclerotic effect, our results may provide mechanistic insight into a series of animal studies that have shown myriocin can potently suppress atherosclerosis (33-37). These findings suggest that disrupting the ABCA1-SPTLC1 complex may represent a novel anti-atherosclerotic therapy.

## Supporting Information

Refer to Web version on PubMed Central for supplementary material.

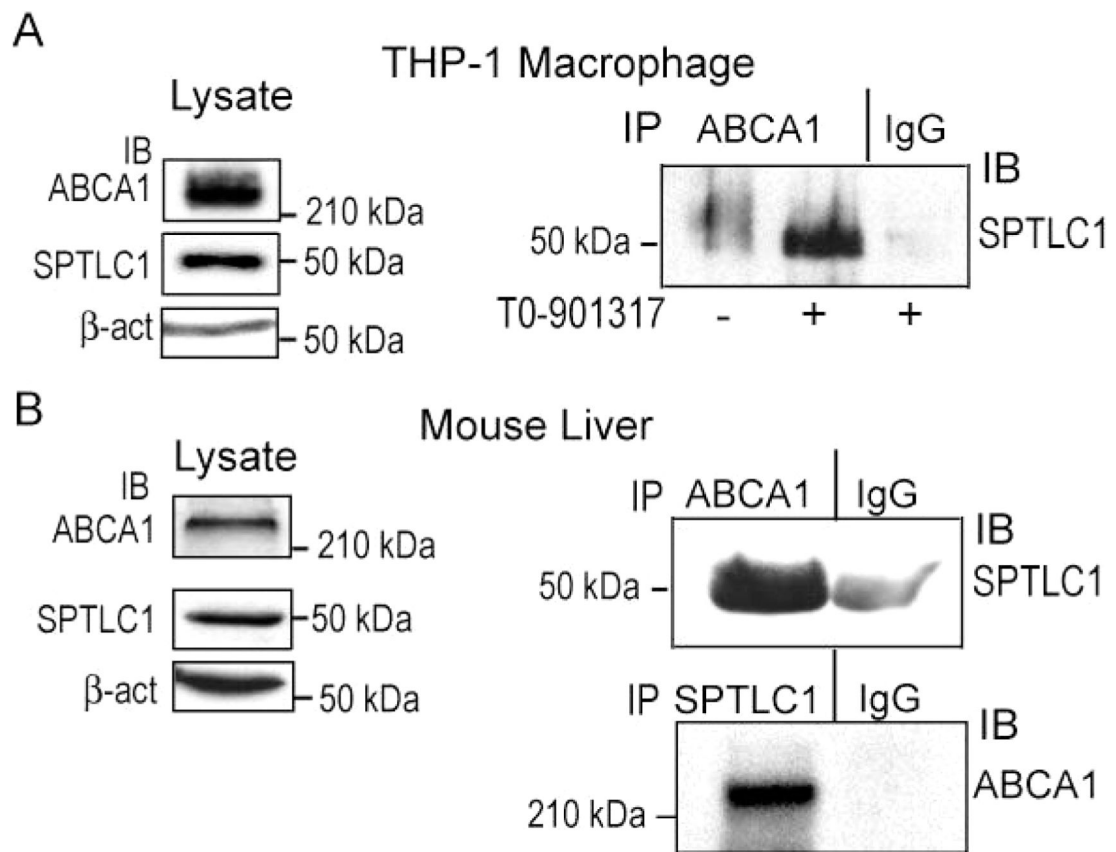
## REFERENCES

1. Maxfield FR, Tabas I. Role of cholesterol and lipid organization in disease. *Nature* 2005;438:612–621. [PubMed: 16319881]
2. Bodzioch M, Orso E, Klucken J, Langmann T, Botcher A, Diederich W, Drobnik W, Barlage S, Buchler C, Porsch-Ozcurumez M, Kaminski WE, Hahmann HW, Oette K, Rothe G, Aslanidis C,

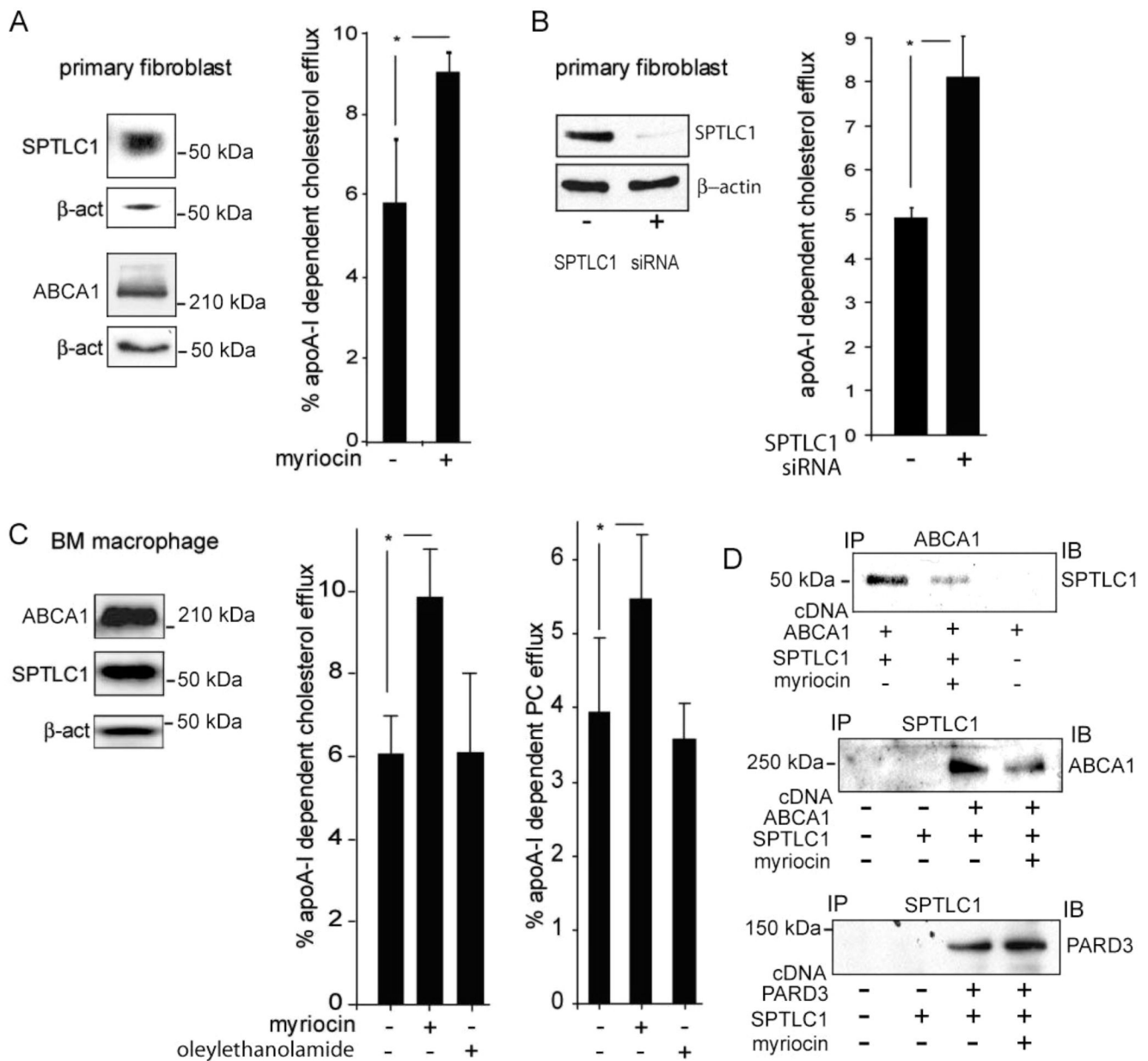
- Lackner KJ, Schmitz G. The gene encoding ATP-binding cassette transporter 1 is mutated in Tangier disease. *Nat. Genet* 1999;22:347–351. [PubMed: 10431237]
3. Brooks-Wilson A, Marcil M, Clee SM, Zhang LH, Roomp K, van Dam M, Yu L, Brewer C, Collins JA, Molhuizen HO, Loubser O, Ouellette BF, Fichter K, Ashbourne-Excoffon KJ, Sensen CW, Scherer S, Mott S, Denis M, Martindale D, Frohlich J, Morgan K, Koop B, Pimstone S, Kastelein JJ, Hayden MR. Mutations in ABC1 in Tangier disease and familial high-density lipoprotein deficiency. *Nat. Genet* 1999;22:336–345. [PubMed: 10431236]
  4. Lawn RM, Wade DP, Garvin MR, Wang X, Schwartz K, Porter JG, Seilhamer JJ, Vaughan AM, Oram JF. The Tangier disease gene product ABC1 controls the cellular apolipoprotein-mediated lipid removal pathway. *J. Clin. Invest* 1999;104:R25–R31. [PubMed: 10525055]
  5. Rust S, Rosier M, Funke H, Real J, Amoura Z, Piette JC, Deleuze JF, Brewer HB, Duverger N, Deneffle P, Assmann G. Tangier disease is caused by mutations in the gene encoding ATP-binding cassette transporter 1. *Nat. Genet* 1999;22:352–355. [PubMed: 10431238]
  6. Joyce CW, Amar MJ, Lambert G, Vaisman BL, Paigen B, Najib-Fruchart J, Hoyt RF Jr, Neufeld ED, Remaley AT, Fredrickson DS, Brewer HB Jr, Santamarina-Fojo S. The ATP binding cassette transporter A1 (ABCA1) modulates the development of aortic atherosclerosis in C57BL/6 and apoE-knockout mice. *Proc. Natl. Acad. Sci. U.S.A* 2002;99:407–412. [PubMed: 11752403]
  7. Singaraja RR, Fievat C, Castro G, James ER, Hennuyer N, Clee SM, Bissada N, Choy JC, Fruchart JC, McManus BM, Staels B, Hayden MR. Increased ABCA1 activity protects against atherosclerosis. *J. Clin. Invest* 2002;110:35–42. [PubMed: 12093886]
  8. van Eck M, Bos IS, Kaminski WE, Orso E, Rothe G, Twisk J, Bottcher A, Van Amersfoort ES, Christiansen-Weber TA, Fung-Leung WP, Van Berkel TJ, Schmitz G. Leukocyte ABCA1 controls susceptibility to atherosclerosis and macrophage recruitment into tissues. *Proc. Natl. Acad. Sci. U.S.A* 2002;99:6298–6303. [PubMed: 11972062]
  9. Zuchner S, Sperfeld AD, Senderek J, Sellhaus B, Hanemann CO, Schroder JM. A novel nonsense mutation in the ABC1 gene causes a severe syringomyelia-like phenotype of Tangier disease. *Brain* 2003;126:920–927. [PubMed: 12615648]
  10. Brousseau ME, Schaefer EJ, Dupuis J, Eustace B, Van Eerdewegh P, Goldkamp AL, Thurston LM, FitzGerald MG, Yasek-McKenna D, O'Neill G, Eberhart GP, Weiffenbach B, Ordovas JM, Freeman MW, Brown RH Jr, Gu JZ. Novel mutations in the gene encoding ATP-binding cassette 1 in four tangier disease kindreds. *J. Lipid Res* 2000;41:433–441. [PubMed: 10706591]
  11. Fitzgerald ML, Okuhira K, Short GF III, Manning JJ, Bell SA, Freeman MW. ATP-binding cassette transporter A1 contains a novel C-terminal VFNFA motif that is required for its cholesterol efflux and ApoA-I binding activities. *J. Biol. Chem* 2004;279:48477–48485. [PubMed: 15347662]
  12. Okuhira K, Fitzgerald ML, Sarracino DA, Manning JJ, Bell SA, Goss JL, Freeman MW. Purification of ATP-binding cassette transporter A1 and associated binding proteins reveals the importance of  $\beta$  1-syntrophin in cholesterol efflux. *J. Biol. Chem* 2005;280:39653–39664. [PubMed: 16192269]
  13. Jiang XC, Paultre F, Pearson TA, Reed RG, Francis CK, Lin M, Berglund L, Tall AR. Plasma sphingomyelin level as a risk factor for coronary artery disease. *Arterioscler., Thromb., Vasc. Biol* 2000;20:2614–2618. [PubMed: 11116061]
  14. Nelson JC, Jiang XC, Tabas I, Tall A, Shea S. Plasma sphingomyelin and subclinical atherosclerosis: Findings from the multi-ethnic study of atherosclerosis. *Am. J. Epidemiol* 2006;163:903–912. [PubMed: 16611667]
  15. Timmins JM, Lee JY, Boudyguina E, Kluckman KD, Brunham LR, Mulya A, Gebre AK, Coutinho JM, Colvin PL, Smith TL, Hayden MR, Maeda N, Parks JS. Targeted inactivation of hepatic Abca1 causes profound hypoalphalipoproteinemia and kidney hypercatabolism of apoA-I. *J. Clin. Invest* 2005;115:1333–1342. [PubMed: 15841208]
  16. Hornemann T, Wei Y, von Eckardstein A. Is the mammalian serine-palmitoyltransferase a high molecular weight complex? *Biochem. J* 2007;405:157–164. [PubMed: 17331073]
  17. Fitzgerald ML, Morris AL, Rhee JS, Andersson LP, Mendez AJ, Freeman MW. Naturally occurring mutations in the largest extracellular loops of ABCA1 can disrupt its direct interaction with apolipoprotein A-I. *J. Biol. Chem* 2002;277:33178–33187. [PubMed: 12084722]

18. Leventhal AR, Chen W, Tall AR, Tabas I. Acid sphingomyelinase-deficient macrophages have defective cholesterol trafficking and efflux. *J. Biol. Chem* 2001;276:44976–44983. [PubMed: 11579092]
19. Nagao K, Takahashi K, Hanada K, Kioka N, Matsuo M, Ueda K. Enhanced apoA-I-dependent cholesterol efflux by ABCA1 from sphingomyelin-deficient CHO cells. *J. Biol. Chem* 2007;282:14868–14874. [PubMed: 17409096]
20. Bejaoui K, Uchida Y, Yasuda S, Ho M, Nishijima M, Brown RH Jr, Holleran WM, Hanada K. Hereditary sensory neuropathy type 1 mutations confer dominant negative effects on serine palmitoyltransferase, critical for sphingolipid synthesis. *J. Clin. Invest* 2002;110:1301–1308. [PubMed: 12417569]
21. McCampbell A, Truong D, Broom DC, Allchorne A, Gable K, Cutler RG, Mattson MP, Woolf CJ, Frosch MP, Harmon JM, Dunn TM, Brown RH Jr. Mutant SPTLC1 dominantly inhibits serine palmitoyltransferase activity in vivo and confers an age-dependent neuropathy. *Hum. Mol. Genet* 2005;14:3507–3521. [PubMed: 16210380]
22. Mujawar Z, Rose H, Morrow MP, Pushkarsky T, Dubrovsky L, Mukhamedova N, Fu Y, Dart A, Orenstein JM, Bobryshev YV, Bukrinsky M, Sviridov D. Human immunodeficiency virus impairs reverse cholesterol transport from macrophages. *PLoS Biol* 2006;4:e365. [PubMed: 17076584]
23. Denis M, Landry YD, Zha X. ATP-binding cassette A1-mediated lipidation of apolipoprotein A-I occurs at the plasma membrane and not in the endocytic compartments. *J. Biol. Chem* 2008;283
24. Faulkner LE, Panagotopoulos SE, Johnson JD, Woollett LA, Hui DY, Witting SR, Maiorano JN, Davidson WS. An analysis of the role of a retroendocytosis pathway in ATP-binding cassette transporter (ABCA1)-mediated cholesterol efflux from macrophages. *J. Lipid Res.* 2008
25. Buechler C, Boettcher A, Bared SM, Probst MC, Schmitz G. The carboxyterminus of the ATP-binding cassette transporter A1 interacts with a  $\beta$  2-syntrophin/utrophin complex. *Biochem. Biophys. Res. Commun* 2002;293:759–765. [PubMed: 12054535]
26. Munehira Y, Ohnishi T, Kawamoto S, Furuya A, Shitara K, Imamura M, Yokota T, Takeda S, Amachi T, Matsuo M, Kioka N, Ueda K.  $\alpha$ 1-Syntrophin modulates turnover of ABCA1. *J. Biol. Chem* 2004;279:15091–15095. [PubMed: 14722086]
27. Hanada K. Serine palmitoyltransferase, a key enzyme of sphingolipid metabolism. *Biochim. Biophys. Acta* 2003;1632:16–30. [PubMed: 12782147]
28. Cox JS, Chapman RE, Walter P. The unfolded protein response coordinates the production of endoplasmic reticulum protein and endoplasmic reticulum membrane. *Mol. Biol. Cell* 1997;8:1805–1814. [PubMed: 9307975]
29. Sriburi R, Bommiasamy H, Buldak GL, Robbins GR, Frank M, Jackowski S, Brewer JW. Coordinate regulation of phospholipid biosynthesis and secretory pathway gene expression in XBP-1(S)-induced endoplasmic reticulum biogenesis. *J. Biol. Chem* 2007;282:7024–7034. [PubMed: 17213183]
30. Meier KD, Deloche O, Kajiwara K, Funato K, Riezman H. Sphingoid base is required for translation initiation during heat stress in *Saccharomyces cerevisiae*. *Mol. Biol. Cell* 2006;17:1164–1175. [PubMed: 16381812]
31. Fagone P, Sriburi R, Ward-Chapman C, Frank M, Wang J, Gunter C, Brewer JW, Jackowski S. Phospholipid biosynthesis program underlying membrane expansion during B-lymphocyte differentiation. *J. Biol. Chem* 2007;282:7591–7605. [PubMed: 17213195]
32. Feng B, Tabas I. ABCA1-mediated cholesterol efflux is defective in free cholesterol-loaded macrophages. Mechanism involves enhanced ABCA1 degradation in a process requiring full NPC1 activity. *J. Biol. Chem* 2002;277:43271–43280. [PubMed: 12215451]
33. Glaros EN, Kim WS, Quinn CM, Jessup W, Rye KA, Garner B. Myriocin slows progression of established atherosclerotic lesions in apolipoprotein-E gene knockout mice. *J. Lipid Res* 2007;49:324–331. [PubMed: 17978313]
34. Glaros EN, Kim WS, Wu BJ, Suarna C, Quinn CM, Rye KA, Stocker R, Jessup W, Garner B. Inhibition of atherosclerosis by the serine palmitoyl transferase inhibitor myriocin is associated with reduced plasma glycosphingolipid concentration. *Biochem. Pharmacol* 2007;73:1340–1346. [PubMed: 17239824]

35. Hojjati MR, Li Z, Zhou H, Tang S, Huan C, Ooi E, Lu S, Jiang XC. Effect of myriocin on plasma sphingolipid metabolism and atherosclerosis in apoE-deficient mice. *J. Biol. Chem* 2005;280:10284–10289. [PubMed: 15590644]
36. Park TS, Panek RL, Mueller SB, Hanselman JC, Rosebury WS, Robertson AW, Kindt EK, Homan R, Karathanasis SK, Rekhter MD. Inhibition of sphingomyelin synthesis reduces atherogenesis in apolipoprotein E-knockout mice. *Circulation* 2004;110:3465–3471. [PubMed: 15545514]
37. Park TS, Panek RL, Rekhter MD, Mueller SB, Rosebury WS, Robertson A, Hanselman JC, Kindt E, Homan R, Karathanasis SK. Modulation of lipoprotein metabolism by inhibition of sphingomyelin synthesis in ApoE knockout mice. *Atherosclerosis* 2006;189:264–272. [PubMed: 16458317]

**FIGURE 1.**

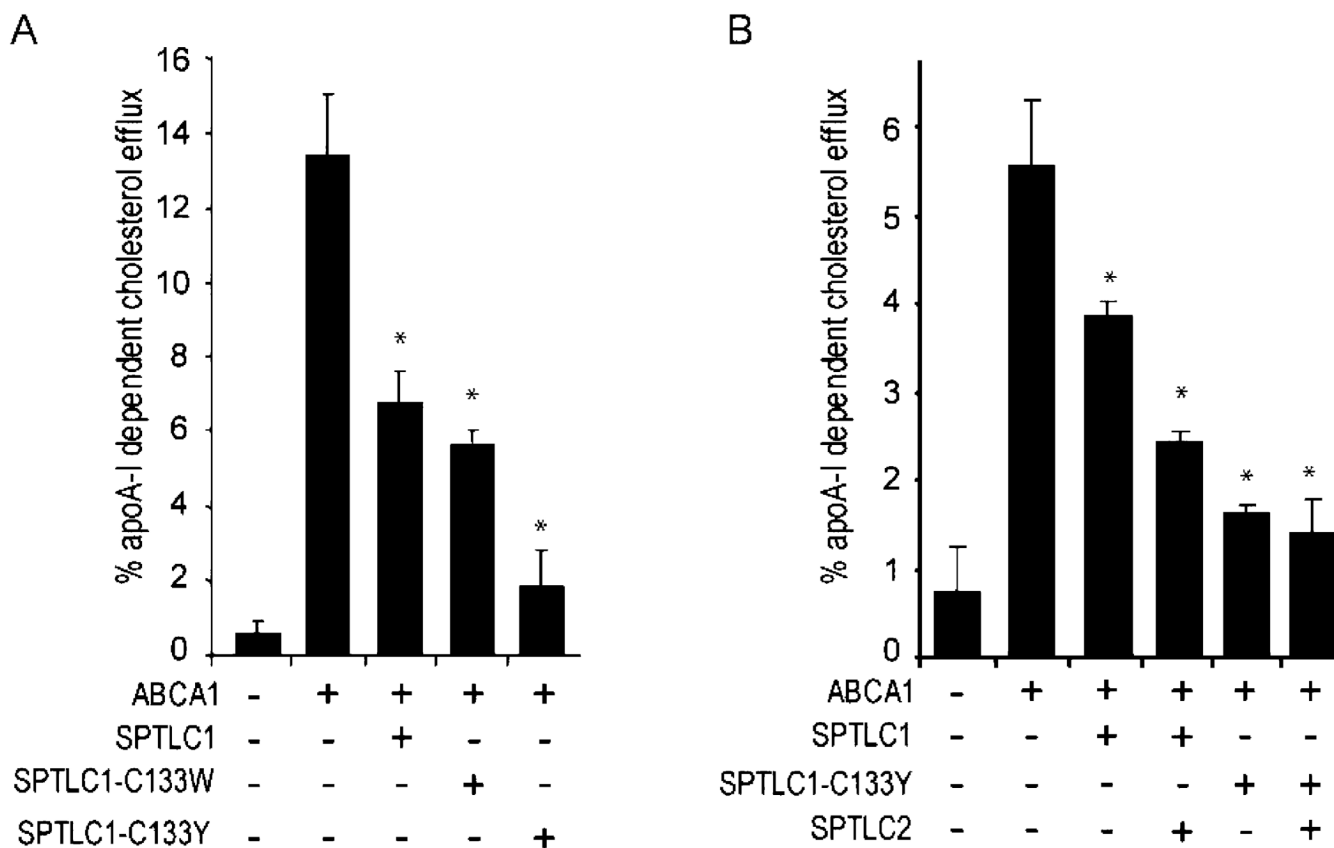
ABCA1 and SPTLC1 interact at physiologic expression levels in macrophages and in the liver. (A) Human THP-1 macrophages differentiated with PMA (100 nM, 72 h) and treated with LXR agonist T0-901317 (10  $\mu$ M, 24 h) express both ABCA1 and SPTLC1 as determined by immunoblotting (left panels). ABCA1 and SPTLC1 form a protein complex as determined by immunoprecipitation of lysates with an anti-ABCA1 antibody, or an equivalent amount of nonimmune IgG, from differentiated cells treated or not with T0-901317 and immunoblotted for the presence of SPTLC1 in the precipitates (right panel). (B) ABCA1 and SPTLC1 are expressed in mouse liver and interact as determined by immunoblotting (left panels) and immunoprecipitation with an anti-ABCA1 antibody (top right panel) or with an anti-SPTLC1 antibody (bottom right panel).

**FIGURE 2.**

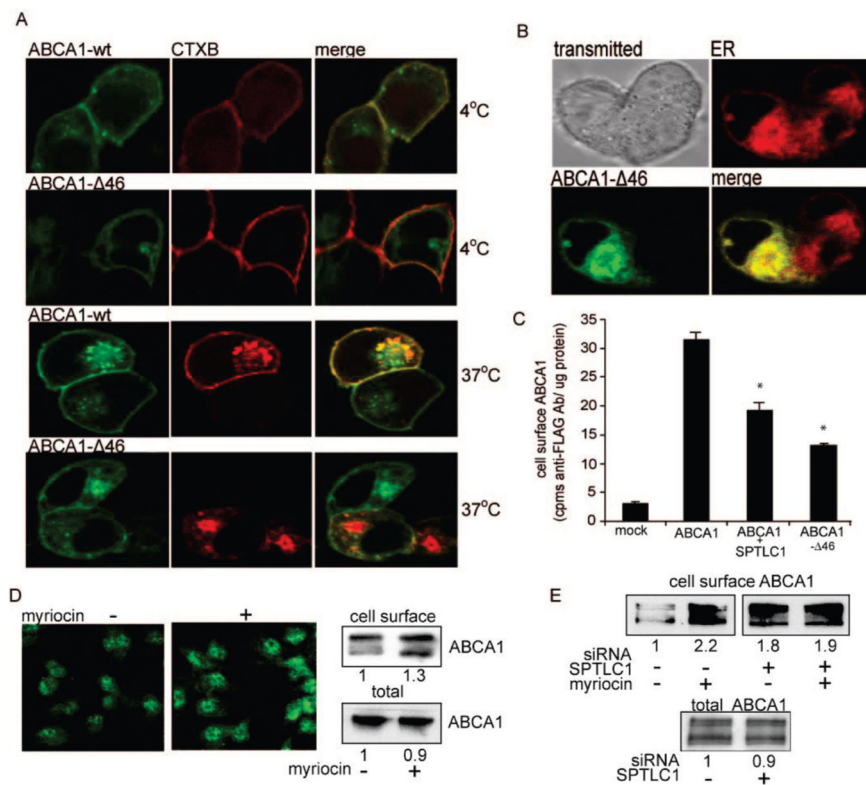
SPTLC1 inhibition with myriocin or by siRNA knockdown increases the rate of ABCA1 efflux. (A) Primary human fibroblasts express ABCA1 and SPTLC1 as determined by immunoblotting (left panel). Inhibition of fibroblast SPTLC1 function either with myriocin (a specific SPTLC1 inhibitor) or by siRNA knockdown significantly increased the rate of ABCA1-dependent cholesterol efflux to apoA-I (graphs in panels A and B). (C) Primary mouse bone marrow-derived macrophages express ABCA1 and SPTLC1 and when treated with myriocin (10  $\mu$ M) but not oleylethanolamide (10  $\mu$ M, a related long chain base ceramidase inhibitor) significantly increase the rates of both cholesterol and phosphatidylcholine efflux to apoA-I. (D) Myriocin (10  $\mu$ M) disrupts the ABCA1-SPTLC1 interaction as determined by immunoprecipitation of FLAG-tagged ABCA1 (top panel) or FLAG-tagged SPTLC1 (middle panel) out of 293ET cells co-expressing untagged SPTLC1 or ABCA1, respectively. In contrast, myriocin does not disrupt the SPTLC1-PARD3 interaction as determined by

immunoprecipitation of FLAG-tagged SPTLC1 out of cells co-expressing PARD3 (bottom panel). All efflux measures were performed in triplicate ( $\pm$ standard deviation) and are representative of two or more assays [(\*)  $P < 0.05$ ].

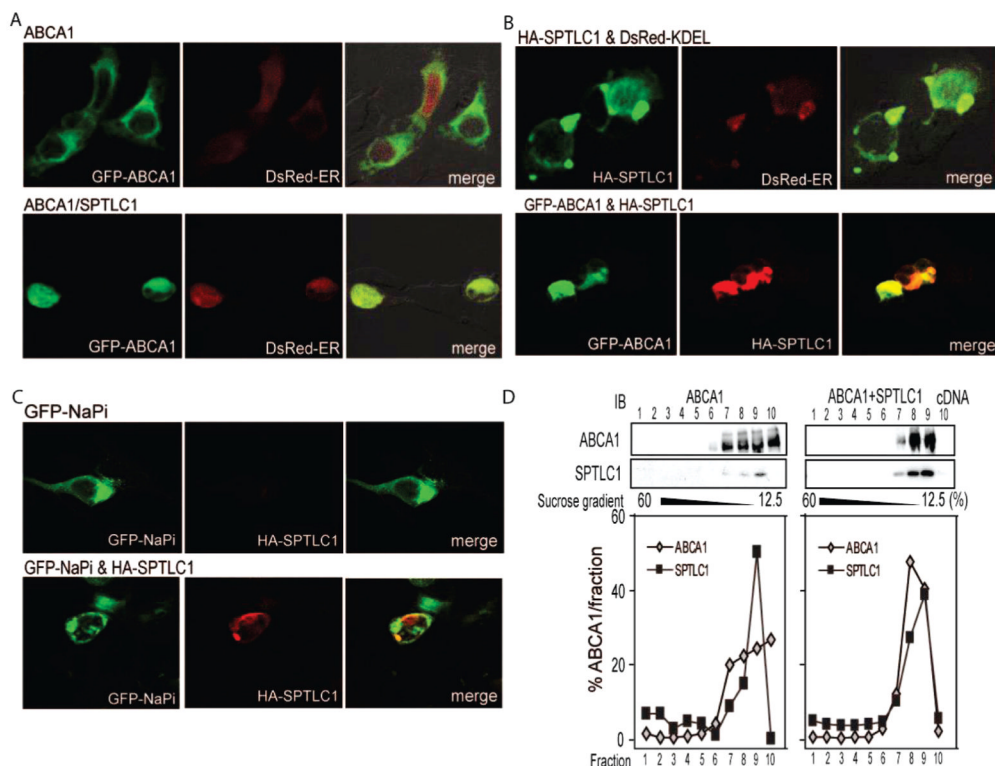


**FIGURE 3.**

Dominant-negative SPTLC1 mutants still inhibit ABCA1 cholesterol efflux. (A) ApoA-I-dependent cholesterol efflux was assessed in 293-ET cells transfected with ABCA1 cDNA alone or in the presence of SPTLC1, SPTLC1-C133W, and SPTLC1-C133Y cDNA. (B) The ability of SPTLC1 and the SPTLC1-C133Y mutant to inhibit ABCA1 cholesterol efflux is not blocked by the co-expression of SPTLC2. All cholesterol efflux measures were performed in triplicate [ $\pm$ standard deviation; (\*)  $P < 0.05$ , vs ABCA1 alone] and are representative of two or more assays.

**FIGURE 4.**

The C-Terminus of ABCA1 is required for the exit of ABCA1 from the ER, and SPTLC1 reduces the level of ABCA1 cell surface expression. (A) Vital confocal microscopy was used to colocalize in 293 cells wild-type GFP-ABCA1 (ABCA1-wt) or the GFP-ABCA1-Δ46 mutant with the B subunit of cholera toxin (CTXB). At 4 °C, CTXB binds cell surface gangliosides but is not internalized and prominently colocalizes with ABCA1-wt but not the Δ46 mutant. At 37 °C, CTXB moves to the Golgi compartment where there is still significant colocalization with ABCA1-wt but not the Δ46 mutant. (B) The Δ46 mutant is trapped in the endoplasmic reticulum as evidenced by its strong colocalization with an ER specific lipid dye. (C) Co-expression of SPTLC1 with ABCA1 in 293 cells significantly reduces the level of cell surface expression of a FLAG-ABCA1 transporter nearly to the extent that the ABCA1 C-terminal Δ46 mutation does as determined by a radio-immunoassay. Graphed is the amount of cell surface binding of an anti-FLAG antibody to 293 cells transfected with empty vector, the FLAG-ABCA1 cDNA, with or without the SPTLC1 cDNA, or with the FLAG-ABCA1-Δ46 cDNA [ $n = 3$ ,  $\pm$ standard deviation; (\*)  $P < 0.01$  vs ABCA1 alone]. (D) Inhibition of bone marrow macrophage SPTLC1 with myriocin (10  $\mu$ M) increases the level of endogenous cell surface ABCA1 as determined by immunofluorescence microscopy of nonpermeabilized cells (left panels) and by biotinylation of cell surface proteins (top right panels; densitometry values of duplicate samples are given). Myriocin did not increase total ABCA1 protein levels (bottom right panels). (E) siRNA knockdown of THP-1 SPTLC1 increases basal levels of cell surface ABCA1 and blunts the myriocin effect but does not increase total ABCA1 protein levels.

**FIGURE 5.**

SPTLC1 blocks the exit of ABCA1 from the ER. (A) SPTLC1 traps ABCA1 in the ER as evidenced by the strong colocalization of GFP-ABCA1 with a DsRed fusion protein carrying the calreticulin KDEL ER targeting sequence when expressed in the presence of SPTLC1 (bottom panels). GFP-ABCA1 expressed alone does not colocalize with the DsRed ER signal (top panels). (B) As expected, immunofluorescent localization of HA-tagged SPTLC1 showed it also colocalized with the DsRed ER protein (top panels) and with the trapped GFP-ABCA1 (bottom panels). (C) SPTLC1 expression does not alter the localization of the sodium phosphate transporter as indicated by the lack of colocalization of a GFP-NaP<sub>1</sub> transporter with HA-SPTLC1. (D) Sucrose gradient fractionation confirms SPTLC1 altered the distribution of ABCA1 in 293ET cells such that a greater percent of ABCA1 cofractionates with SPTLC1 in the ER. Immunoblots of the distribution of ABCA1 and SPTLC1 across the gradient are shown, and graphed is the percent distribution of ABCA1 and SPTLC1 in each fraction.